

## Short-lived radionuclide production cross sections calculated by the Liège intranuclear cascade model

Deye Tao 

Department of Physics, Nanjing University, Nanjing 210093, China  
Key Laboratory of Dark Matter and Space Astronomy, Purple Mountain Observatory, CAS, Nanjing 210023, China

Tiekuang Dong\*

Key Laboratory of Dark Matter and Space Astronomy, Purple Mountain Observatory, CAS, Nanjing 210023, China

Sujun Yun

School of Electronic Engineering, Nanjing Xiaozhuang University, Nanjing 211171, China

Zhongzhou Ren<sup>†</sup>

School of Physics Science and Engineering, Tongji University, Shanghai 200092, China



(Received 18 January 2021; accepted 18 March 2021; published 12 April 2021)

In this paper, we calculate the cross sections for proton-induced reactions producing short-lived radionuclides like  ${}^7,{}^{10}\text{Be}$ ,  ${}^{26}\text{Al}$ ,  ${}^{53,54}\text{Mn}$ , etc., with the Liège intranuclear cascade model (INCL++). The results show that the INCL model, when coupled with the proper deexcitation model, gives satisfactory results for most of the considered reactions. Generally, results for reactions with  $(\Delta N - \Delta Z)$  equal to 0 or 1 are more likely to precisely match experimental data than those for reactions with larger or smaller  $|\Delta N - \Delta Z|$ . Our results can provide useful references for both the users and developers of INCL and deexcitation models.

DOI: [10.1103/PhysRevC.103.044606](https://doi.org/10.1103/PhysRevC.103.044606)

### I. INTRODUCTION

The short-lived radionuclides (SLRs) are a class of extinct nuclides that have been proposed to be produced in the very early stage of the solar system [1]. The existence of these nuclei has been confirmed by their decay daughters found in the calcium-aluminum-rich inclusions, the oldest solids in the solar system wrapped in some kind of meteorites like chondrites [2]. As a consequence, researches on the exact production process of SLRs are of great significance in helping us to see more details in the evolutionary history of the solar system.

The production cross sections are crucial input parameters to derive the theoretical content of SLRs produced by early solar activities [1,3–5]. However, most of the reactions occurring near the protosun to produce SLRs require energy that is too high to realize in laboratories, which causes difficulty in measuring the relevant cross sections experimentally. It is the reason that there are quite few cross-section data available. Therefore, it is necessary to find a way of simulating the high-energy reactions and to obtain the cross sections theoretically.

The Liège intranuclear cascade (INCL) model [6] was first developed in 1983 to study reactions between heavy ions [7], and now is widely used in simulations of nucleon- and light-ion-induced spallation reactions. According to the benchmark of spallation models [8] organized by the International Atomic

Energy Agency, the combination of the INCL model and deexcitation model ABLA07 is one of the most accurate models. In 2016, Chen *et al.* [9] calculated the cross sections for proton- and neutron-induced spallation reactions producing  ${}^3\text{He}$ ,  ${}^{10}\text{Be}$ , and  ${}^{26}\text{Al}$  by the INCL model and obtained acceptable results. However, the systematical calculation of SLRs-production cross sections and analytical comparisons with experiments and between results from different deexcitation models are rather rare.

In this paper, we combined the latest version of the INCL model, INCL++ v6.29, with three different deexcitation models to evaluate the SLRs-production cross sections for proton-induced spallation reactions, and compared results with experimental data to test the validity of INCL++ and the three deexcitation models.

### II. MODEL DESCRIPTION

#### A. INCL

The INCL model is based on the idea that at a sufficiently high incident energy the nucleon-nucleus reactions can be treated as a series of independent nucleon-nucleon binary interactions within a common mean-field potential [6,10].

According to the framework of the model [6,11,12], incident particles, assumed to be traveling along straight-line trajectories, initiate a series of binary collisions in the target nucleus, followed by possible emissions of nucleons, pions, and light clusters. Among the collisions taking place in a

\*tkdong@pmo.ac.cn

†zren@tongji.edu.cn

spherical calculation volume, inelastic collisions

$$NN \Rightarrow N\Delta, \quad \Delta \Rightarrow \pi N \quad (1)$$

cause the production and absorption of  $\Delta$ 's and pions. Calculations are performed relativistically and effects like Pauli blocking and Coulomb deviation are considered. The reactions come to an end when the remnant system reaches a state of thermalization, parametrized by the self-consistently determined cascade stopping time. One of the prominent advantages of the INCL model is that there is no adjustable parameter. All the parameters used are determined either phenomenally or once for all.

During the last decades, the application range of the INCL model has been widely extended. For the latest INCL++ version, the projectiles could be nucleons, pions, or the newly added light ions with the mass number below 18. The upper energy limit is up to 15–20 GeV for pion-, kaon-, and nucleon-induced reactions, and a few GeV for light-ion-induced reactions [13–15]. Although the concept of cascade reaction is proposed for spallation reactions with the incident energy larger than 100 MeV [16], INCL could give acceptable results in the energy of tens of MeV [8].

### B. Deexcitation

The INCL model addresses the reaction system until a thermalization is established, leaving the remnant in an approximately equilibrate state characterized by its mass, charge, excitation energy, and angular momentum. To obtain the observable final state, information of the remnant system will be delivered to the following deexcitation model, which statistically describes the cooling down of the excited nucleus. Deexcitation models could differ from each other in the ways of tackling specific processes like evaporation, fission, multifragmentation and/or other kinds of breakup, through which the remnant deexcites. In this paper, we employed three deexcitation models ABLA v3p, GEMINI++, and SMM [17], in addition to the Fermi breakup model. The Fermi breakup model is set by INCL as the default deexcitation model for excited nuclei with mass numbers less than 16.

### III. RESULTS AND DISCUSSIONS

With the models discussed above, we calculated cross sections for reactions producing SLRs including  ${}^{7,10}\text{Be}$ ,  ${}^{14}\text{C}$ ,  ${}^{22}\text{Na}$ ,  ${}^{26}\text{Al}$ ,  ${}^{44}\text{Ti}$ , and  ${}^{53,54}\text{Mn}$  from their parents. The calculated SLRs and the corresponding parent elements are listed in Table I. And for comparison, we coupled INCL++, respectively, to three different deexcitation models, namely, ABLA v3p, GEMINI++, and SMM, during calculations. Some of the calculated cross sections for SLRs-producing reactions are shown in Figs. 1–5. In the incident-energy range of 60–3000 MeV, most of the results are in good agreement with experimental data within a factor of 2 for at least one adopted deexcitation model.

To reveal the rules under which the calculated results are affected by the reactions, we evaluated for all modeled reactions the parameters  $(\Delta N - \Delta Z)$  and  $\Delta N/\Delta Z$ , which explicitly characterize a reaction. Approximately, for most of

TABLE I. The calculated SLRs and the accordant target elements.

Isotope	Target elements
Be-7,10	Be, B, C, O
C-14	O
Na-22	Na, Mg, Al, Si
Al-26	Mg, Al, Si
Ti-44	Ti, Fe
Mn-53,54	Mn, Fe, Ni

the reactions with  $(\Delta N - \Delta Z)$  equal to 0 or 1, good simulated results are produced, and the results given by different deexcitation models show good consistency (within a factor of 2) with each other. A large proportion of calculated results for this kind of reactions exhibit matching shape with experimental data and results from other models (Fig. 1). The calculated results for reactions  ${}^{55}\text{Mn}(p, pn) {}^{54}\text{Mn}$  and  ${}^{\text{nat}}\text{Fe}(p, x) {}^{53}\text{Mn}$  are nearly perfect in fitting the experimental data regardless of the deexcitation model coupled. For reactions

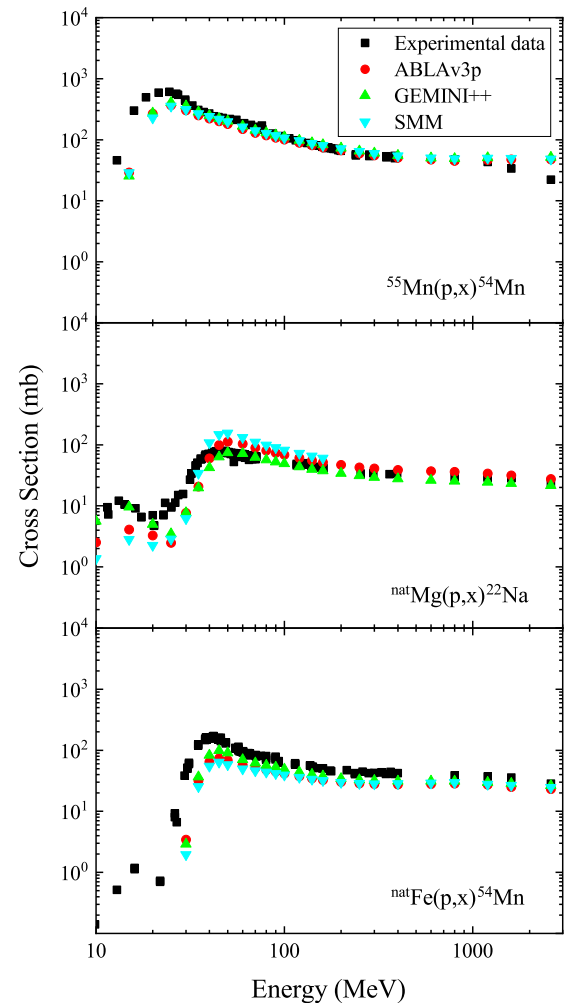


FIG. 1. The calculated cross sections for  ${}^{55}\text{Mn}(p, pn) {}^{54}\text{Mn}$ ,  ${}^{\text{nat}}\text{Mg}(p, x) {}^{22}\text{Na}$ , and  ${}^{\text{nat}}\text{Fe}(p, x) {}^{54}\text{Mn}$ . The experimental data are taken from Ref. [18].

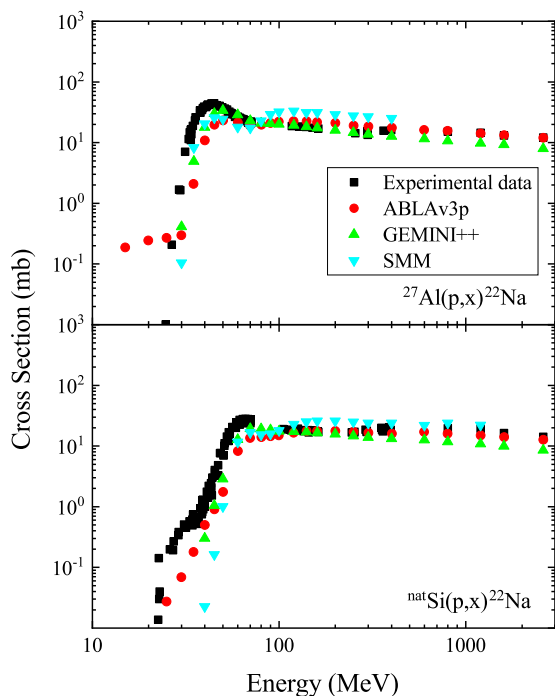


FIG. 2. The calculated cross sections for  $^{27}\text{Al}(p, x)^{22}\text{Na}$  and  $^{\text{nat}}\text{Si}(p, x)^{22}\text{Na}$ . The experimental data are taken from Ref. [18].

$^{\text{nat}}\text{Mg}(p, x)^{22}\text{Na}$ ,  $^{27}\text{Al}(p, x)^{26}\text{Al}$ , and  $^{\text{nat}}\text{Si}(p, x)^{26}\text{Al}$ , precisely fitted results within the considered energy range of 60–3000 MeV are produced by GEMINI++, and results from other models are close to experimental data but slightly overestimated (within a factor of 3). On the other hand, the results of  $^{\text{nat}}\text{Fe}(p, x)^{54}\text{Mn}$  obtained by GEMINI++ are in good agreement with experimental data and those by other models are slightly underestimated (within a factor of 2). However, for reactions  $^{23}\text{Na}(p, x)^{22}\text{Na}$ ,  $^{27}\text{Al}(p, x)^{22}\text{Na}$ , and  $^{\text{nat}}\text{Si}(p, x)^{22}\text{Na}$ , the shapes of calculated results deviate slightly from experimental data and results from other models, but precisely agreeable results are reproduced in some energies by a specific deexcitation model (Fig. 2).

In contrast, when the value of  $|\Delta N - \Delta Z|$  is larger than 1, the calculated results are more likely to show a severer deviation from experimental data in shape and/or value, and the consistency between different deexcitation models is also reduced (Fig. 3). Some results have only accordant shape with experimental data and each other, such as reactions  $^{\text{nat}}\text{Mg}(p, x)^{26}\text{Al}$  and  $^{\text{nat}}\text{Ni}(p, x)^{54}\text{Mn}$ . The magnitudes of these results are either overestimated or underestimated. For the other reactions, however, results from different models disagree with experimental data and each other not only in magnitude but also in shape, like the reactions producing  $^7\text{Be}$ . Moreover, in the simulation for reaction  $^{\text{nat}}\text{O}(p, x)^{14}\text{C}$ , INCL and its coupled deexcitation models failed severely, the calculated cross sections showing a drastic deviation from experimental data of a factor of at most 4 in higher energies for all the used deexcitation models.

Based on the results shown above, we can predict approximately the performance of INCL and deexcitation models in calculating cross sections according to the values of  $(\Delta N - \Delta Z)$

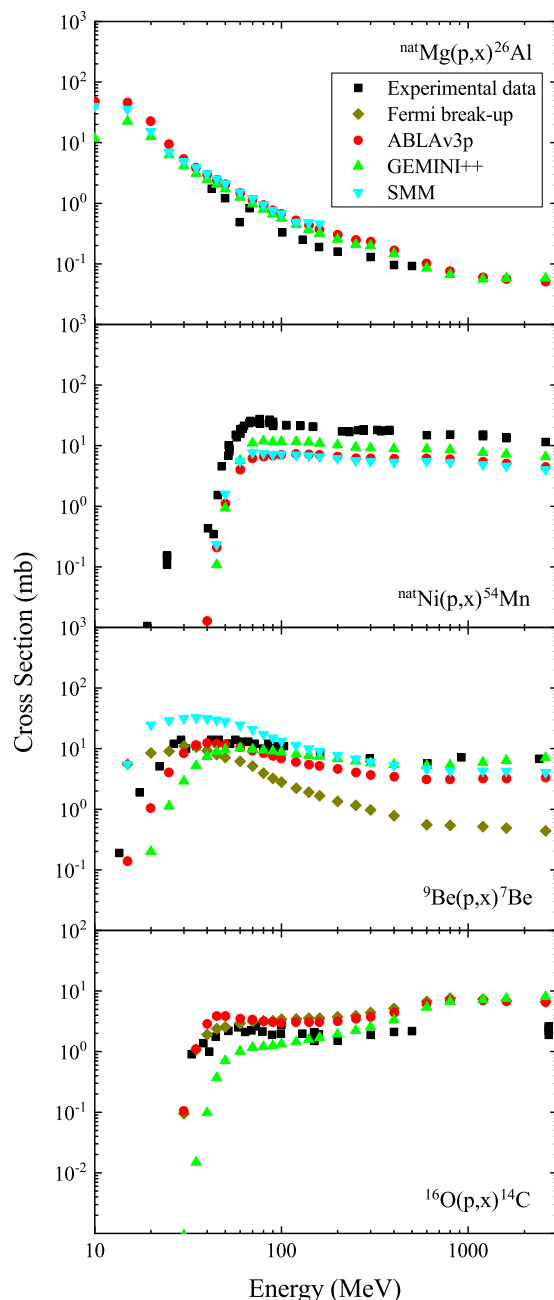


FIG. 3. The calculated cross sections for  $^{\text{nat}}\text{Mg}(p, x)^{26}\text{Al}$ ,  $^{\text{nat}}\text{Ni}(p, x)^{54}\text{Mn}$ ,  $^9\text{Be}(p, x)^7\text{Be}$ , and  $^{\text{nat}}\text{O}(p, x)^{14}\text{C}$ . The experimental data are taken from Refs. [18–23].

for simulated reactions. But exceptions exist, for these are only qualitative conclusions. For reactions  $^{\text{nat}}\text{C}(p, x)^7\text{Be}$  and  $^{\text{nat}}\text{O}(p, x)^7\text{Be}$ , the parameter  $(\Delta N - \Delta Z)$  is equal to 1 but the calculated results from the three adopted deexcitation models are not satisfying (Fig. 4). However, we can exclude these exceptions because these two reactions have relatively light targets, which are more suitable to be assigned to the Fermi breakup model, and the consequent results are within a factor of 2. On the other hand, among reactions with larger  $|\Delta N - \Delta Z|$ , acceptable results are produced for  $^{\text{nat}}\text{Ti}(p, x)^{44}\text{Ti}$  by SMM, but the disagreement between results from different deexcitation models is still large (Fig. 5).

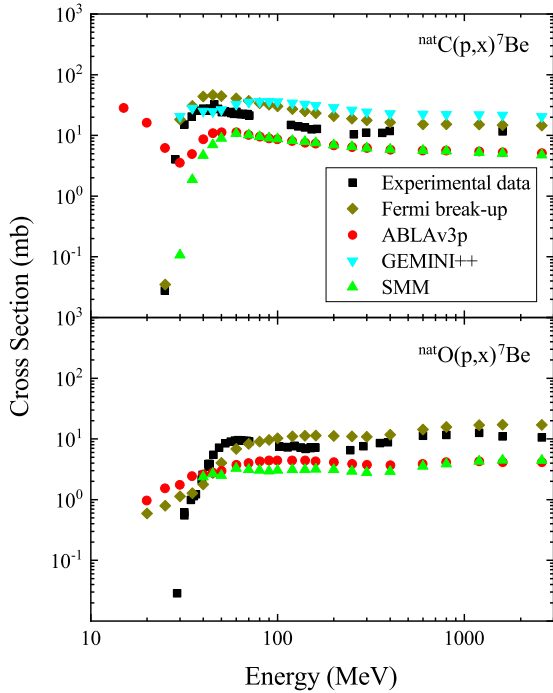


FIG. 4. The calculated cross sections for  ${}^{\text{nat}}\text{C}(p, x) {}^7\text{Be}$  and  ${}^{\text{nat}}\text{O}(p, x) {}^7\text{Be}$ . The experimental data are taken from Ref. [18].

From the above results we can see that the performance of INCL++ and deexcitation models in calculating cross sections depends not only on the reaction, but also on the specific deexcitation model. Among the adopted deexcitation models, the GEMINI++ model shows an obvious advantage in reproducing the cross sections for SLRs-production reactions, by giving the most appropriate results on its own for 11 reactions in 20 in total. For the reactions  ${}^9\text{Be}(p, x) {}^7\text{Be}$ ,  ${}^{\text{nat}}\text{Mg}(p, x) {}^{22}\text{Na}$ ,  ${}^{\text{nat}}\text{Si}(p, x) {}^{26}\text{Al}$ , and  ${}^{\text{nat}}\text{Fe}(p, x) {}^{54}\text{Mn}$ , GEMINI++ obtained precisely fitted results while the others made a deviation larger than a factor of 1.5. Besides, the results of  ${}^{\text{nat}}\text{C}(p, x) {}^{10}\text{Be}$  can only be simulated by GEMINI++ to have an accordant shape with experiments.

SMM performed a perfect simulation for reaction  ${}^{\text{nat}}\text{Ti}(p, x) {}^{44}\text{Ti}$ , while the other models overestimated the values by at least a factor of 2. Also, for another reaction

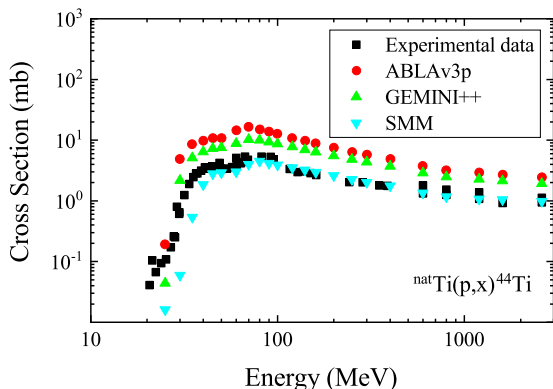


FIG. 5. The calculated cross sections for  ${}^{\text{nat}}\text{Ti}(p, x) {}^{44}\text{Ti}$ . The experimental data are taken from Ref. [18].

producing  ${}^{44}\text{Ti}$ ,  ${}^{\text{nat}}\text{Fe}(p, x) {}^{44}\text{Ti}$ , SMM gives best-simulated values again. But some calculations cannot be accomplished, when coupled to SMM, for reactions the target elements of which lie between oxygen and silicon in the periodic table. Especially for reactions where the oxygen nuclei are targets, the simulations break down for all the considered energies.

There are also two reactions the cross sections of which are well reproduced by two models, GEMINI++ and ABLAv3p, respectively, in different energy ranges. Cross sections for  ${}^{27}\text{Al}(p, x) {}^{22}\text{Na}$  are precisely calculated in the energy range 50–300 MeV by GEMINI++, and 400–3000 MeV by ABLAv3p. As a similar situation, the reaction  ${}^{\text{nat}}\text{Si}(p, x) {}^{22}\text{Na}$  also received good simulated results from these two models, respectively, in different energy ranges. Such a situation, although it makes no sense for calculating well-fitted values, inspires us about the nature of such reactions according to the methods or assumptions used in models giving better results. Besides, it also suggests the proper scopes of application of different deexcitation models.

The INCL++ set the Fermi breakup model, which specializes in simulations of light nuclei, as the default deexcitation model for nuclei with mass numbers no more than 16. In order to explicitly study the performance of each model, and to research the capability of the Fermi breakup model, we also calculated the results by coupling INCL++ to the Fermi breakup model for reactions where the targets are not heavier than oxygen. The results show that, compared with the other three deexcitation models, the Fermi breakup model indeed has an advantage in dealing with reactions producing light SLRs. But discrepancies between results and experimental data are still large.

#### IV. SUMMARY

The SLRs-production cross sections for some reactions from normal elements are calculated by INCL++ coupled with three different deexcitation models. The results show that for most reactions INCL++ could give acceptable predictions when coupled to the proper deexcitation model. Generally speaking, for reactions with  $(\Delta N - \Delta Z)$  equal to 0 or 1, the calculated results are more likely to be in good agreement with experimental data regardless of the deexcitation model involved. And for more than half of the calculated reactions the most appropriate results are produced by the deexcitation model GEMINI++ coupled with INCL++. However, more discrepancies arise between calculated results and experimental data for reactions with  $|\Delta N - \Delta Z|$  larger than 1. And results are also not very satisfactory for reactions producing light SLRs like  ${}^{7,10}\text{Be}$  and  ${}^{14}\text{C}$ . For these aspects, a further improvement of the INCL++ and deexcitation models is needed in the future.

#### ACKNOWLEDGMENTS

This work is supported by the National Natural Science Foundation of China (Grants No. 12035011, No. 11805103, No. U1738205, No. 11673075, No. 11975167, and No. 11761161001). We also thank D. Mancusi for providing us the INCL++ v6.29 code.

- [1] T. Lee, F. H. Shu, H. Shang, A. E. Glassgold, and K. E. Rehm, *Astrophys. J.* **506**, 898 (1998).
- [2] K. D. McKeegan, M. Chaussidon, and F. Robert, *Science* **289**, 1334 (2000).
- [3] M. Gounelle, F. H. Shu, H. Shang, A. E. Glassgold, K. E. Rehm, and T. Lee, *Astrophys. J.* **548**, 1051 (2001).
- [4] I. Leya, A. N. Halliday, and R. Wieler, *Astrophys. J.* **594**, 605 (2003).
- [5] P. A. Sossi, F. Moynier, M. Chaussidon, J. Villeneuve, C. Kato, and M. Gounelle, *Nat. Astron.* **1**, 0055 (2017).
- [6] D. Mancusi, A. Boudard, J. Cugnon, J. C. David, P. Kaitaniemi, and S. Leray, *Phys. Rev. C* **90**, 054602 (2014).
- [7] J. Cugnon, T. Mizutani, and J. Vandermeulen, *Nucl. Phys. A* **352**, 505 (1981).
- [8] S. Leray, J. C. David, M. Khandaker, G. Mank, A. Mengoni, N. Otsuka, D. Filges, F. Gallmeier, A. Konobeyev, and R. Michel, *J. Korean Phys. Soc.* **59**, 791 (2011).
- [9] J. Chen, T. K. Dong, and Z. Z. Ren, *Phys. Rev. C* **93**, 064608 (2016).
- [10] V. E. Bunakov and G. V. Matvejev, *Z. Phys. A* **322**, 511 (1985).
- [11] A. Boudard, J. Cugnon, J. C. David, S. Leray, and D. Mancusi, *Phys. Rev. C* **87**, 014606 (2013).
- [12] A. Boudard, J. Cugnon, S. Leray, and C. Volant, *Phys. Rev. C* **66**, 044615 (2002).
- [13] S. Pedoux and J. Cugnon, *Nucl. Phys. A* **866**, 16 (2011).
- [14] S. Pedoux, Extension of the Liège intranuclear cascade model to the 2-15 GeV incident energy range, Ph.D. thesis, University of Liège, 2011.
- [15] J. Hirtz, J. C. David, A. Boudard, J. Cugnon, S. Leray, I. Leya, and D. Mancusi, *Eur. Phys. J. Plus* **133**, 436 (2018).
- [16] R. Serber, *Phys. Rev.* **72**, 1114 (1947).
- [17] D. Filges, S. Leray, Y. Yariv, A. Mengoni, A. Stanculescu, and G. Mank, Joint ICTP-IAEA advanced workshop on model codes for spallation reactions, International Atomic Energy Agency Report, INDC(NDS)-0530, 2008.
- [18] R. Michel and N. Otsuka, Database for proton induced residual production cross sections up to 2.6 GeV, International Atomic Energy Agency Report, INDC(GER)-0052, 2014.
- [19] J. M. Sisterson, K. Kim, A. Beverding, P. A. J. Englert, M. W. Caffee, J. Vincent, C. Castaneda, and R. C. Reedy, Measuring excitation functions needed to interpret cosmogenic nuclide production in lunar rocks, in *Application of Accelerators in Research and Industry: Proceedings of the Fourteenth International Conference, Parts 1 and 2*, edited by J. L. Duggan and I. L. Morgan, AIP Conf. Proc. No. 392 (AIP, New York, 1997), pp. 811–814.
- [20] V. Aleksandrov, M. Semenova, and V. Semenov, *Vopr. At. Nauki Tekh., Ser.: Yad.-Fiz. Issled.* **8**, 16 (1990).
- [21] M. Barbier and S. Regnier, *J. Inorg. Nucl. Chem.* **33**, 2720 (1971).
- [22] A. J. T. Jull, S. Cloudt, D. J. Donahue, J. M. Sisterson, R. C. Reedy, and J. Masarik, *Geochim. Cosmochim. Acta* **62**, 3025 (1998).
- [23] M. Tamers and G. Delibrias, *C. R. Hebd. Seances Acad. Sci.* **253**, 1202 (1961).